Electronic stopping power from first-principles calculations with account for core electron excitations and projectile ionization

Ari Ojanperä,[1] Arkady V. Krasheninnikov,[1,2] and Martti Puska[1]
[1]*COMP Centre of Excellence, Department of Applied Physics, Aalto University, P.O. Box 11100, FI-00076 AALTO, Finland*
[2]*Materials Physics Division, University of Helsinki, P.O. Box 43, FI-00014, Finland*
(Received 26 March 2013; revised manuscript received 22 November 2013; published 14 January 2014)

We use Ehrenfest dynamics and time-dependent density functional theory to calculate electronic stopping power S_e of energetic ions in graphitic targets from first principles. By treating core electrons as valence electrons within the projected augmented wave framework, we demonstrate that this approach provides an accurate description of S_e for a wide range of ions and ion energies, even when not only valence, but also core electron excitations are essential. Our impact-parameter-dependent approach capable of describing the stopping of both low- and high-energy ions is a significant step forward in S_e calculations, as it makes it possible to monitor projectile charge state during impacts, estimate contributions of core and valence electron excitations to S_e, and it gives a quantitative description of electronic stopping in the cross-over region for bulk solids and nanostructures from first principles.

DOI: 10.1103/PhysRevB.89.035120 PACS number(s): 61.80.−x, 34.20.−b, 34.50.Bw, 61.85.+p

I. INTRODUCTION

The development of the time-dependent density functional theory (TDDFT)[1–3] and computational techniques[4–7] accounting for the correlated dynamics of electrons and nuclei have made quantitative studies of nonadiabatic processes in molecules and solids possible. Among these methods, the combination of the Ehrenfest dynamics (ED; see Ref. 4 for an overview) and TDDFT has been shown to provide useful insights into a broad range of physical phenomena, such as excited carrier dynamics,[8] structure transformations and dissociation in photoexcited systems,[9,10] or low-energy collisions between atoms and molecules,[11] which involve either the decay of the excited system back to the ground state or nuclear-electron coupling-induced excitations. Within this approach, the nuclei evolve on an effective potential representing an average over the adiabatic electronic states weighted by their state populations.

Simulations of atom motion combined with the TDDFT have also been used to study the response of solids to ion irradiation. In particular, the amount of energy deposited into electronic excitations under impacts of energetic ions[12–17] and fragmentation of nanostructures due to the combination of electronic and vibronic excitations[18] have been addressed. Insights into the dependence of the electronic stopping power S_e on projectile velocity have been obtained with the explicit account for the atomic structure of the target, such as an explanation for the anomalous stopping of light ions in gold,[13] oscillatory dependence of S_e on projectile atomic number Z for slow ions,[19] and how correlations between electronic and nuclear stopping affect defect production at the initial stages of radiation damage.[12] However, pseudopotentials have been used in all previous first-principles studies, and core electrons have not explicitly been taken into account, so that simulations have been limited to cases of either low-velocity or low-mass projectiles, which did not involve core electron excitations in the colliding atoms. Moreover, none of the analytical and semianalytical theories (for an overview, see Refs. 20–22) of electronic stopping can describe both slow and fast ions (as compared to the core electron Bohr velocities in atoms involved). Thus, the development of an approach that could give an accurate first-principles description of both limits is highly desirable, as it should provide quantitative results in the crossover region and make it possible to estimate the contribution of each process into S_e.

In this work, by calculating S_e in graphitic targets as a function of projectile energy E_I, we demonstrate that the TDDFT-ED approach when used together with the projector augmented wave (PAW) formalism[23] can describe electronic stopping for a wide range of projectile types and energies. In the most common implementations of the PAW method, core states are frozen. However, by treating core electrons as valence electrons, the method can describe changes in the core states, which is essential for simulating core electron excitations.[24] Here, we call this approach the pseudoatom (PA) method. The calculated S_e is in a very good agreement with the experimental data, and the position of the maximum in the $S_e(E_I)$ curve matches well the experimental one, justifying our method. More important, the TDDFT-ED approach combined with the PA formalism drastically improves the description of the stopping process as compared to the ordinary PAW method, providing an *ab initio* technique for calculating S_e at high energies, at which core electron excitations become essential.

II. CALCULATION METHOD AND SIMULATION SETUP

We employed TDDFT-ED as implemented in the real-space code GPAW.[25,26] The real-space implementation of S_e calculations has several advantages over the plane-wave[15] and atomic orbital[12,16] approaches, as it makes it possible to use any boundary conditions and does not require the introduction of ghost orbitals along the ion path. Moreover, parallelization in real-space is straightforward and efficient. Our implementation of the TDDFT-ED scheme is thoroughly described in a previous paper,[26] and hence here we give only the details important for the present study. We would like to stress that the application of the TDDFT-ED approach to S_e calculations is motivated by the very nature of the problem.

Indeed, (i) high-energy ions have well-defined trajectories, hence their motion can be treated classically; (ii) the mean-field approach generally works well for solids, in which there are many close-lying electronic states; (iii) as we are only interested in energy deposition (not in energy conversion to phonons and defects), which occurs on a femtosecond time scale, the accurate account for the de-excitation mechanism is not required.

We chose graphene as the target because it is the most important carbon allotrope, being the parent material for graphite, fullerenes, and carbon nanotubes. Moreover, there is plenty of experimental data available for carbon targets. Most of the calculations used 5 × 5 supercells containing 50 carbon atoms, but we also performed calculations with supercells of 128 atoms and obtained essentially the same results. Besides, calculations for AA-stacked slabs composed from up to 6 stacked graphene layers containing 50 atoms each were carried out. We used periodic boundary conditions in all three dimensions. The spacing of the real-space grids was 0.2 Å in all calculations. Simulations with smaller grids gave essentially the same results.

Unless mentioned otherwise, the projectiles were initially singly ionized. The initial state for the TDDFT-ED simulations was obtained from the ground-state DFT calculation.[27] Then, a kinetic energy E_I was assigned to the projectile with its velocity being perpendicular to the graphene target. The key quantity of interest was the energy deposited into the target, which can be converted to S_e using the thickness of the target. In order to compare with experimental results for graphite, the target thickness was chosen as the graphite interlayer spacing (or its multiple). The deposited energy was calculated as the difference between the projectile kinetic energies half a graphite interlayer before and after passing through the target.

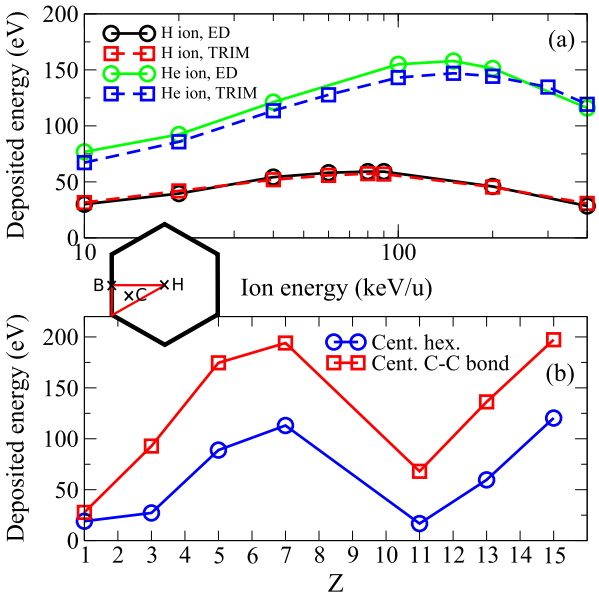

FIG. 1. (Color online) (a) Energy deposited into the graphene target for H and He ions as a function of initial projectile energy. The ED values represent an estimated average over the graphene surface. The TRIM results represent experimental data averaged over graphite targets. (b) Energy deposited into the graphene target as a function of nuclear charge Z of the projectile. The results are shown for two different trajectories: through the center of the hexagon (H) and the center of a C-C bond (B). The lines are guides to the eye. The inset shows these impact points and the centroid of the triangle (C).

III. RESULTS AND DISCUSSIONS

A. Stopping of light projectiles without core electrons

First, we investigated the collision of light ions with a single graphene sheet. We calculated the spatially averaged deposited energy[28] for hydrogen (H^+) and helium (He^{2+}) ions as functions of E_I by taking into account the symmetry of the lattice and restricting the calculations to the triangle shown in the inset of Fig. 1. The results of the calculations, along with the results obtained using the TRIM code,[29] which represent experimental data averaged over various carbon targets, are shown in Fig. 1(a). The deposited energy for protons matches the TRIM and thus the experimental values presented in the Supplemental Material[30] very well in a wide range of energies. Our calculations also agree with the previous theoretical results for graphene fragments[14] and correctly predict the position of the maximum on the curve, which is associated with the velocity-matching effect, a resonance in the classical sense when projectile residence time near the atom matches the orbital period of the electron. The agreement for the He ion is also good, but the TDDFT values are slightly higher than those given by TRIM. The agreement between the PAW results and the experimental data indicates that core electron excitations in the target atoms under impacts of H and He projectiles are not important. Indeed, the relatively high values of projectile energies ($E_I \sim 130$ and 520 keV for H and He ions, respectively), at which the maximum kinetic energy transferred to an electron[31] is comparable to core state energy $E_{1s} \sim 285$ eV for the sp^2-hybridized carbon, indicate that the contribution of core excitations in target atoms is small.

B. Deposited energy as a function of nuclear charge for slow projectiles

We extended the test of our approach to heavier singly ionized projectiles ranging from Li to P by calculating S_e in the limit of low ion energies using the ordinary PAW method. The deposited energy is presented in Fig. 1(b) as a function of the nuclear charge Z. Projectile velocities in experiments have varied typically between 0.2 and 0.8 a.u., while we chose the velocity to be 0.63 a.u., which corresponds to a kinetic energy of 10 keV for a proton. By comparing the calculated data to those presented in Refs. 32 and 33, it is evident that TDDFT-ED with PAW reproduces the experimentally observed behavior, i.e., oscillating S_e as a function of nuclear charge, which is associated with the electronic shell structure of the projectiles and their sizes.[20,32,33] Using the models of scattering theory and resonance levels in solids, the peaks in S_e can be understood to arise from resonant states in the conduction band, while the minima are related to the formation of closed shells.[32] Moreover, our results agree well with those obtained previously using TDDFT-ED method based on pseudopotentials.[19]

C. Stopping of projectiles with account for core electron excitations

Thus far, the predictive power of our TDDFT-ED calculations has turned out to be very good. However, we have hitherto studied electronic stopping in cases, in which the effects of core electron excitations on S_e are not significant. The next and most important step in this work was to investigate, using the pseudoatom method, situations in which these effects are strong. Within the PA approach, by calculating projectors and partial waves, the all-electron wave functions can be reconstructed from the pseudo ones also for the core states.[24]

First, we calculated S_e for Li ions, as Li 1s level is not very deep, so that one can expect that core electrons of the projectile to play a significant role in the stopping process. In our simulations, the Li 1s energy level was −58.5 eV. We carried out calculations for the Li ion at various impact energies using either the PA method for the Li or the ordinary frozen-core PAWs for all atoms. We chose the centroid of the triangle (C) shown in the inset in Fig. 1 as our impact point, since it gives a rough estimate for the average deposited energy.[28] We note that the energy lost by the ion in this case includes the energy deposited into the excitation of the projectile electrons and projectile ionization.

The results are presented in Fig. 2(a). We considered two initial charge states ($Z_0 = 1$; $Z_0 = 2$) within the PA approach. The core electron excitations of the Li projectile turned out to have a major effect on S_e: the frozen-core curve starts to significantly deviate from the experimental data when E_I exceeded 40 keV/u. At the same time, using the PA approach for the Li projectile drastically improves the agreement with the experiment.

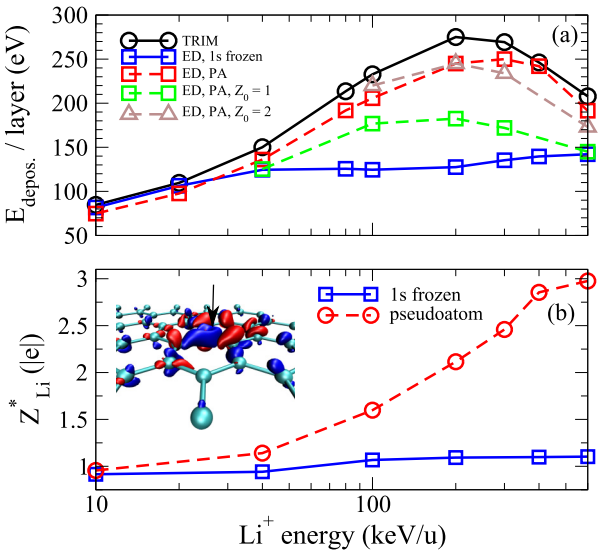

FIG. 2. (Color online) (a) Stopping power of Li ions in graphene targets as a function of the impact energy. The ED values represent an estimate for the average deposited energy. PA denotes the pseudoatom method. The TRIM results are the experimental data averaged over graphitic targets. (b) Projectile charge Z^* at the end of the simulation as a function of impact energy. The charge was estimated from the integrated time-dependent all-electron density around the projectile. The lines are guides to the eye. The inset shows the difference between the PA and frozen-core densities just after the projectile has passed through the target for $E_{\text{ion}} = 200$ keV/u and the centroid impact point. The red and blue colors correspond to increase and decrease in density, respectively, and the isosurface value is 0.005 a.u.

In order to better understand the difference between the frozen-core and PA results for Li, we calculated the projectile charge state Z^* just before and after collision with graphene sheet by integrating the time-dependent all-electron density around the projectile. The integration radius was chosen to be 3 Å, as it gives 99.9% of the electronic charge for an isolated Li atom in its ground state. We found that Z^* changes by 0.1–0.3 (depending on the impact point and ion energy) during the collision with the graphene sheet, so that one can expect that when penetrating a bulk graphitic target the projectile reaches an averaged "stationary" charge state, which is defined by its energy. This is also evident from Fig. 3(b), where the amount of deposited energy is given for the target composed from a different number of graphene layers. Thus, we also carried out simulations where Z^* before the impact was obtained by the acceleration rate (the red curve),[34] as in Ref. 35. We found a good agreement between the experiments and simulations: the difference between our calculations and the experimental results is not larger than 20% for all the impact energies. This indicates that Z^* has indeed a certain "stationary" charge state when penetrating a bulk target, which is independent of Z_0. Thus, our approach makes it possible to calculate the deposition of energy into a nanosystem of a finite width with account for the original charge state of the projectile and also that in a bulk system. It also allows one to calculate Z^* directly from first principles.

Having analyzed stopping of Li ions, we investigated the applicability of the PA method in the case of heavier projectiles. First, we carried out stopping calculations for Na ions, using two different approaches: (i) keeping the 1s state frozen, while the 2s and 2p states were treated using the PA method and (ii) using the ordinary frozen core PAW approach with everything but 3s states frozen. The impact point was again the centroid of the triangle. Similar to the Li ions, we investigated stopping for both one and three layers of graphene. The results are shown in Fig. 3(a). The frozen-core results deviate significantly from the experiments even at the lowest considered projectile energy. Using the PA approach for the projectile again drastically improves the agreement between simulation and experiment. While the simulations do not reproduce the experimental data perfectly, the deviation in this case is roughly similar to that for the Li ion, confirming the robustness of the PA scheme.

We further studied the dependence of the results on the number of graphene layers in more detail, Fig. 3(b). We focused on the center-of-hexagon trajectory for Li, Na, and Ne projectiles. In the case of Ne and Na, the 1s core state was frozen. For all projectiles, the layer-normalized deposited energy decreases with the number of layers, suggesting that the electronic structure of the projectile changes in the collision with the first layer and some energy is deposited into the projectile excitation and ionization. The electronic structure of the projectile does not vary significantly between the layers. Even though the changes in the deposited energy are relatively small, our results indicate that energy deposition into the

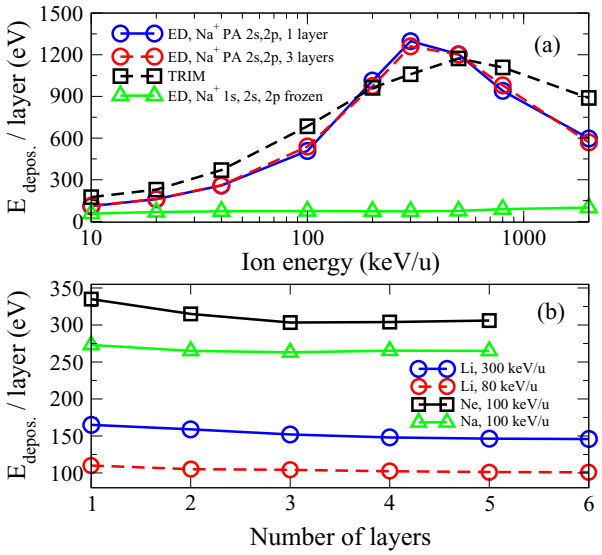

FIG. 3. (Color online) (a) Stopping power of Na ions in graphene as a function of the impact energy. The ED values represent an estimate for the average deposited energy. PA denotes the pseudoatom method. The TRIM curve is the experimental data averaged over carbon targets. (b) Deposited energy per layer obtained with different ions and impact energies as a function of the number of graphene layers. The impact point in all calculations was the center of the hexagon. The lines are guides to the eye.

projectile excitation and ionization should also be accounted for in quantitative calculations of S_e.

As evident from Figs. 2 and 3(a), S_e is underestimated at the highest energies considered. One contributing factor can be excitations of core states in the target, which we have hitherto not taken into account. To investigate this issue, we simulated the collision of nitrogen (N 1*s* level is deeper than that in C) with a graphene sheet. The impact point was chosen to be along the C-C bond 0.4 Å away from the nearest carbon atom, which was treated using the PA method. Our calculations showed that core electron excitations do not play any role until $E_I =$ 300 keV/u. However, at higher energies there is a small but clear (3–7%) contribution to S_e from C core electrons, which would be more pronounced if the impact parameter was even closer to the nearest carbon atom. These results show that for a proper *ab initio* description of the electronic stopping process, especially in the case of heavy ions, the effect of the core electrons in the target should not be ignored.

IV. CONCLUSIONS

In conclusion, by treating core electrons as valence electrons, we demonstrated that TDDFT-ED combined with the PAW-based pseudoatom formalism can provide an accurate impact-parameter-dependent description of the electronic stopping power for a wide range of ions, ion energies, and initial charge states of the projectile. Our results indicate that accounting for core electron excitations in projectile and target atoms is crucial for a quantitative description of the electronic stopping of fast ions in bulk solids and nanostructures. Since none of the analytical and semianalytical theories can describe electronic stopping of both slow and fast ions at the same time, our approach is a significant step forward, as it makes it possible to estimate the contribution of core and valence electron excitations and ionization of the colliding atoms into the stopping power, and it gives a quantitative description of the electronic stopping and charge state of the projectile in the crossover region. Moreover, by extending the simulations to a longer time scale, one can describe the evolution of the atomic structure during the conversion of the deposited energy from electronic to vibronic degrees of freedom for a particular geometry, e.g., as in experiments on cutting graphene by swift heavy ions.[36] Finally, our approach makes it also possible to calculate projectile charge state and deposition of energy and into a nanosystem of finite width with account for the original charge state of the projectile, making a direct comparison to the experimental data[37] possible.

ACKNOWLEDGMENTS

The support by the Academy of Finland through several projects is gratefully acknowledged. We also thank CSC Finland for generous grants of computer time. We further acknowledge the 10,000,000 CPU-hour grant at the PRACE Research Infrastructure resource CURIE supercomputer, which made the research described in this paper possible. We also thank Peter Sigmund, E. Artacho, A. Caro, and D. Sanchez-Portal for discussions.

[1] E. Runge and E. K. U. Gross, Phys. Rev. Lett. **52**, 997 (1984).
[2] K. Yabana and G. F. Bertsch, Phys. Rev. B **54**, 4484 (1996).
[3] M. Petersilka, U. J. Gossmann, and E. K. U. Gross, Phys. Rev. Lett. **76**, 1212 (1996).
[4] D. Marx and J. Hutter, *Ab Initio Molecular Dynamics: Basic Theory and Advanced Methods* (Cambridge University Press, Cambridge, 2009).
[5] S. Meng and E. Kaxiras, J. Chem. Phys. **129**, 054110 (2008).
[6] P. V. Parandekar and J. C. Tully, J. Chem. Phys. **122**, 094102 (2005).
[7] C. F. Craig, W. R. Duncan, and O. V. Prezhdo, Phys. Rev. Lett. **95**, 163001 (2005).
[8] Y. Miyamoto, A. Rubio, and D. Tománek, Phys. Rev. Lett. **97**, 126104 (2006).
[9] Y. Tateyama, N. Oyama, T. Ohno, and Y. Miyamoto, J. Chem. Phys. **124**, 124507 (2006).
[10] W. Liang, C. M. Isborn, and X. Li, J. Phys. Chem. A **113**, 3463 (2009).
[11] C. M. Isborn, X. Li, and J. C. Tully, J. Chem. Phys. **126**, 134307 (2007).
[12] A. A. Correa, J. Kohanoff, E. Artacho, D. Sánchez-Portal, and A. Caro, Phys. Rev. Lett. **108**, 213201 (2012).
[13] M. A. Zeb, J. Kohanoff, D. Sánchez-Portal, A. Arnau, J. I. Juaristi, and E. Artacho, Phys. Rev. Lett. **108**, 225504 (2012).
[14] S. Bubin, B. Wang, S. Pantelides, and K. Varga, Phys. Rev. B **85**, 235435 (2012).

[15] A. V. Krasheninnikov, Y. Miyamoto, and D. Tománek, Phys. Rev. Lett. **99**, 016104 (2007).
[16] J. M. Pruneda, D. Sánchez-Portal, A. Arnau, J. I. Juaristi, and E. Artacho, Phys. Rev. Lett. **99**, 235501 (2007).
[17] D. R. Mason, C. P. Race, M. H. F. Foo, A. P. Horsfield, W. M. C. Foulkes, and A. P. Sutton, New J. Phys. **14**, 073009 (2012).
[18] T. Kunert and R. Schmidt, Phys. Rev. Lett. **86**, 5258 (2001).
[19] R. Hatcher, M. Beck, A. Tackett, and S. T. Pantelides, Phys. Rev. Lett. **100**, 103201 (2008).
[20] M. Nastasi, J. Mayer, and J. Hirvonen, *Ion-Solid Interactions—Fundamentals and Applications* (Cambridge University Press, Cambridge, Great Britain, 1996).
[21] G. Schiwietz, E. Luderer, G. Xiao, and P. L. Grande, Nucl. Instrum. Methods Phys. Res., Sect. B **175–177**, 1 (2001).
[22] G. de M. Azevedo, P. L. Grande, and G. Schiwietz, Nucl. Instrum. Methods Phys. Res., Sect. B **164–165**, 203 (2000).
[23] P. E. Blöchl, Phys. Rev. B **50**, 17953 (1994).
[24] A. Sakko *et al*. (unpublished).
[25] J. Enkovaara *et al*., J. Phys. Condens. Matter. **22**, 253202 (2010).
[26] A. Ojanperä, V. Havu, L. Lehtovaara, and M. Puska, J. Chem. Phys. **136**, 144103 (2012).
[27] In the ground-state calculation, we used an external potential at the projectile, which was switched off for the TDDFT-ED calculations, and a neutralizing background charge.
[28] We used fitting techniques to find an approximative S_e for eight impact points within the triangle shown in the inset of Fig. 1. The spatially averaged deposited energy was then calculated using the fitted S_e. The S_e values for the centroid trajectory (C) very closely matched the more accurately calculated average.
[29] J. F. Ziegler and J. P. Biersack, Computer code TRIM (http://www.srim.org, 2011).
[30] See Supplemental Material at http://link.aps.org/supplemental/10.1103/PhysRevB.89.035120 for experimental values.
[31] The maximum kinetic energy $T_{\max}$ can be estimated using the nonrelativistic binary-collision formula $T_{\max} \sim 4m_e E_1/M_1$, where m_e and M_1 are the electron and projectile (ion) mass, respectively.
[32] M. J. Puska and R. M. Nieminen, Phys. Rev. B **27**, 6121 (1983).
[33] P. M. Echenique, R. M. Nieminen, J. C. Ashley, and R. H. Ritchie, Phys. Rev. A **33**, 897 (1986).
[34] In the nonadiabatic ED, the acceleration of the atom (nucleus) gives rise to its partial ionization as the electron density is excited and "lags" behind.
[35] Y. Miyamoto and H. Zhang, Phys. Rev. B **77**, 045433 (2008).
[36] S. Akcöltekin, H. Bukowska, T. Peters, O. Osmani, I. Monnet, I. Alzaher, B. Ban d'Etat, H. Lebius, and M. Schleberger, Appl. Phys. Lett. **98**, 103103 (2011).
[37] R. Ritter, R. A. Wilhelm, M. Stöger-Pollack, R. Heller, A. Mücklich, U. Werner, H. Vieker, A. Beyer, S. Facsko, A. Gölzhäuser, and F. Aumayer, Appl. Phys. Lett. **102**, 063112 (2013).